JOURNAL OF APPLIED ELECTROCHEMISTRY 13 (1983) 295–306

Anodic characteristics of amorphous ternary palladium-phosphorus alloys containing ruthenium, rhodium, iridium, or platinum in a hot concentrated sodium chloride solution

M. HARA*, K. HASHIMOTO, T. MASUMOTO

The Research Institute for Iron, Steel and Other Metals, Tohoku University, Sendai 980, Japan

Received 14 May 1982

Amorphous ternary palladium-based alloys containing platinum group metals as an additional element were prepared by rapid quenching from the molten state and their anodic characteristics were investigated in a 4 mol dm^{-3} NaCl solution of pH 4 and 80° C. The amorphous alloys containing sufficient quantities of rhodium, platinum or iridium were passivated by anodic polarization and their corrosion rates at high current densities in the chlorine evolution region were extremely low. This fact was attributed to the formation of a highly protective passive film due to both the transformation to the amorphous structure and the addition of rhodium, platinum or iridium. The electrocatalytic activities for chlorine evolution of amorphous alloys were higher than those of pure platinum group metals except palladium. In particular, the amorphous $Pd_{41}Ir_{40}P_{19}$ alloy had the desired stable, high electrocatalytic activity for chlorine evolution and the high overvoltage for oxygen evolution.

1. Introduction

Amorphous alloys prepared by rapid quenching from the liquid state are novel metallic materials with various unusual and attractive properties: they always have high mechanical strength (approaching theoretical strength) and considerable toughness; many are soft ferromagnets. Their chemical properties are also unique, some of them are extraordinarily corrosion-resistant. The amorphous alloys are characterized by their single phase nature, even though the alloys with the same composition are solidified without rapid quenching into crystalline multiple phases with poor mechanical properties (low strength and sometimes brittleness). Using the excellent characteristics of the amorphous alloys recent studies have considered them as catalysts for hydrogenation of carbon monoxide [1–3] and as methanol fuel electrodes [4].

Highly efficient anodes for industrial electrolysis are required to possess good electronic conductivity, high chemical stability, high catalytic activity and selectivity, sufficient mechanical strength, etc. [5, 6]. The easiest way to obtain materials possessing such specific properties is the modification of their composition, providing a stable phase with sufficient mechanical strength is formed. For this purpose, the amorphous alloys are suitable since a single phase alloy with complicated composition is easily obtained. The anode for electrolysis of sodium chloride solutions is required to have high catalytic activity for chlorine evolution and low activity for parasitic oxygen evolution along with resistance to corrosion in an extremely aggressive environment. Although the anodic characteristics of platinum group metals in sodium chloride solutions have been extensively studied [7–10], those metals have not been used in the chlor alkali industry because none combine the activity and the corrosion resistance.

In the chlor-alkali industry, many cell houses based on mercury cells were converted to the diaphragm process to avoid water pollution; these

* Present address: Department of Metallurgy, Mining College, Akita University, Akita 010, Japan.

0021–891X/83 $03.00 + .12.

have widely used an anode consisting of an oxide mixture of ruthenium and titanium supported by metallic titanium, known as the dimensionally stable anode (DSA). DSA is an effective anode with high activity for chlorine evolution and sufficient corrosion resistance. One of the problems of using DSA for the electrolysis of sodium chloride solution in the diaphragm process is relatively high oxygen content in the chlorine [11]. This is attributable to a low overvoltage at ruthenium oxide for oxygen evolution [12]. For instance, in the operation of the diaphragm process using a sodium chloride solution, pH 3–4, the oxygen content in the chlorine produced on DSA is reported as 3–3.5 vol %. According to Kolotyrkin [13], the oxygen content in the chlorine produced on DSA in the laboratory experiment was 0.1 vol% at pH 1.7 and the Tafel slope for oxygen evolution was 0.051 V decade^{-1}. This oxygen content is significantly lower. However, a decrease in the solution pH below 3 in industrial electrolysis is not advisable because of damage to the DSA. In contrast to the equilibrium potential for chlorine evolution which is independent of the solution pH, the equilibrium potential for oxygen decreases by 0.059 V with a unit pH increase. Accordingly, when a constant voltage is used for electrolysis of sodium chloride solution, increasing the pH from 1.7 to 3–4 leads to a rise in the overvoltage for oxygen evolution of 0.077–0.136 V, and hence to a remarkable increase in the current density for oxygen evolution (if the mechanism for oxygen evolution is not changed by the pH increase).

On the other hand, when the solid polymer electrolyte cell [14] is adopted in the chlor alkali industry, it may be difficult to use oxide electrodes prepared by the current procedures. It is, therefore, pertinent to investigate the anodic characteristics of new metallic materials, that is, the amorphous alloys in hot concentrated sodium chloride solutions. It is well known that some amorphous alloys have extremely high corrosion resistance, even in acidic chloride environments [15–20]. Among crystalline platinum group metals, palladium is known to have very high activity for chlorine evolution and low activity for oxygen evolution, but it is rapidly corroded in hot concentrated sodium chloride solutions [12]. On the other hand, some palladium alloys easily become amorphous by rapid quenching from the liquid state [21]. The present authors [22, 23] recently reported that amorphous Pd–Ti–P alloys have a high corrosion resistance during anodic polarization in sodium chloride solutions due to the formation of a titanium-enriched passive film but a lower electrocatalytic activity for chlorine evolution than pure palladium.

The present work has been undertaken to prepare amorphous ternary palladium–phosphorus alloys containing ruthenium, rhodium, iridium or platinum for the purpose of improving the corrosion resistance of palladium without harming its superior electrode characteristics for electrolysis of sodium chloride solutions.

2. Experimental

2.1. *Preparation of alloys*

Alloy ingots were prepared as follows: Prescribed amounts of palladium chips and red phosphorus were vacuum-sealed in a quartz ampoule so that the palladium chips were on the red phosphorus, the reaction of phosphorus with palladium was carried out at 400° C for 2 days. Then the temperature was gradually raised to melt the palladium phosphide for homogenization. The palladium phosphide was then melted with various amounts of ruthenium, rhodium, iridium, platinum or silicon under an argon atmosphere, the alloy ingots were prepared by sucking the melt into a quartz tube and subsequent water-quenching. A binary palladium-silicon alloy ingot was similarly prepared by melting palladium and silicon under an argon atmosphere. After the ingot was remelted in a quartz tube under an argon atmosphere, a jet of the molten alloy was impinged by pressurized argon gas onto the outer surface of a rapidly rotating wheel. By this method amorphous alloy ribbons of 0.6–1.5 mm width and 10–30 μm thickness were prepared. Crystalline pure ruthenium, rhodium, palladium, iridium and platinum sheets of about 1.0 mm width and 0.1–0.5 mm thickness were also prepared for comparison. Prior to electrochemical measurements, the amorphous alloy ribbons and metal sheets were cut into about 15 mm lengths and polished with emery paper, degreased

ultrasonically in acetone and finally dried in air. The ruthenium dioxide electrode supported by titanium (RuO_2/Ti) was also prepared for comparison by a literature method [24] (repetitive (× 10) brushing of $RuCl_3$–HCl–isopropanol on a titanium sheet 20 × 2.0 × 0.2 mm^3, evaporating the solvent and heating at 350° C for 10 min in air, and final heating for 2 h at 450° C in air).

2.2. *Anodic polarization measurements*

Potentiostatic polarization measurements were carried out to investigate the active dissolution–passivation behaviour. Galvanostatic polarization curves were also measured for comparing the electrocatalytic activities of the alloys for gas evolution. The potentiostatic polarization curves were measured by polarization for 120 s at each potential and a step-wise change by 0.05 V. The galvanostatic polarization curves were measured by polarization for 300 s at each current density. Corrections for ohmic drop were made by the current interrupter method. 4 mol dm^{-3} NaCl solution of pH 4 was mainly used as the electrolyte. 1 mol dm^{-3} Na_2SO_4 solution of pH 4 was also used to investigate the oxygen overvoltage of the alloys. The pH of these solutions was adjusted by adding 4 mol dm^{-3} HCl and 0.05 mol dm^{-3} H_2SO_4, respectively. These solutions were prepared from reagent grade chemicals and de-ionized water. During measurements, the electrolyte was open to the air and kept at 80° C. An H-type electrolytic cell was used, in which the anode and cathode compartments were separated by an asbestos diaphragm. The solution volume of each compartment was about 1.5 × 10^{-4} m^3. A platinum gauze and a saturated calomel electrode were used as counter and reference electrodes, respectively.

2.3. *Corrosion rate measurements*

Alloy specimens spot-welded with a titanium wire of 0.1 mm diameter and 25 mm length were used for the corrosion rate measurement. When an insulator coating was applied to expose a fixed area of the specimen to the solution, prolonged polarization led to an erroneous result due to the degradation of the coating by chlorine. Accordingly, a certain area of the specimen was directly immersed into the solution without coating. The corrosion rate was estimated from the weight loss after galvanostatic polarization for 25 h at 1000 Am^{-2}. The weight of specimens was measured by a microbalance. When the specimens dissolved vigorously, the measurement time was made shorter. The electrolyte and electrolytic cell used were the same as those for the anodic polarization measurement. The pH of the solution in the anode compartment was measured after the corrosion test.

3. Results

3.1. *Corrosion resistance*

Figure 1 shows potentiostatic anodic polarization curves for amorphous $Pd_{80}Si_{20}$ and $Pd_{81}P_{19}$ alloys measured in 4 mol dm^{-3} NaCl solution of pH 4 and 80° C. The polarization curve for crystalline pure palladium is also shown for comparison. All these specimens exhibited high current densities and dissolved rapidly in the active region. It was, therefore, impossible to measure their anodic polarization curves in the potential region higher than about 0.7 V (SCE). The anodic current density of amorphous $Pd_{81}P_{19}$ alloy is lower than those of pure palladium and amorphous $Pd_{80}Si_{20}$ alloy. It is known that the corrosion resistance of amorphous metal-metalloid alloys was generally improved by addition of a

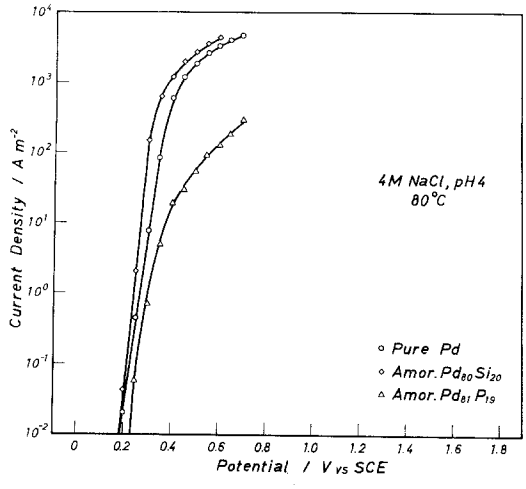

Fig. 1. Potentiostatic anodic polarization curves of pure palladium and amorphous $Pd_{80}Si_{20}$ and $Pd_{81}P_{19}$ alloys measured in 4 mol dm^{-3} NaCl solution of pH 4 and 80° C.

second metallic element [18]. Furthermore, phosphorus was the most effective metalloid additive in improving the corrosion resistance by favouring passivation [24, 25]. Accordingly, an attempt was made to improve the corrosion resistance of the amorphous Pd–P alloy by the addition of platinum group metals as the second metallic element.

Figure 2 shows potentiostatic anodic polarization curves of amorphous palladium-phosphorus alloys with ruthenium, rhodium, platinum or iridium measured in 4 mol dm^{-3} NaCl solution of pH 4 and 80° C. The number in the figure denotes the content of additional platinum group elements in at %. In general, when the active current density was high, the solution in the vicinity of the specimen turned brown due to active dissolution of the alloy. Figure 2 (a) shows that an increase in the ruthenium content of amorphous $Pd_{81-x}Ru_xP_{19}$ alloys slightly decreases the current density in the active region. However, even if the alloy contains 40 at % ruthenium, anodic passivation is not observed. On the other hand, as shown in Figs. 2(b) and (c), the alloys containing 20 at % or more rhodium or 30 at % or more platinum are passivated by anodic polarization and show a subsequent steep rise in the current density due

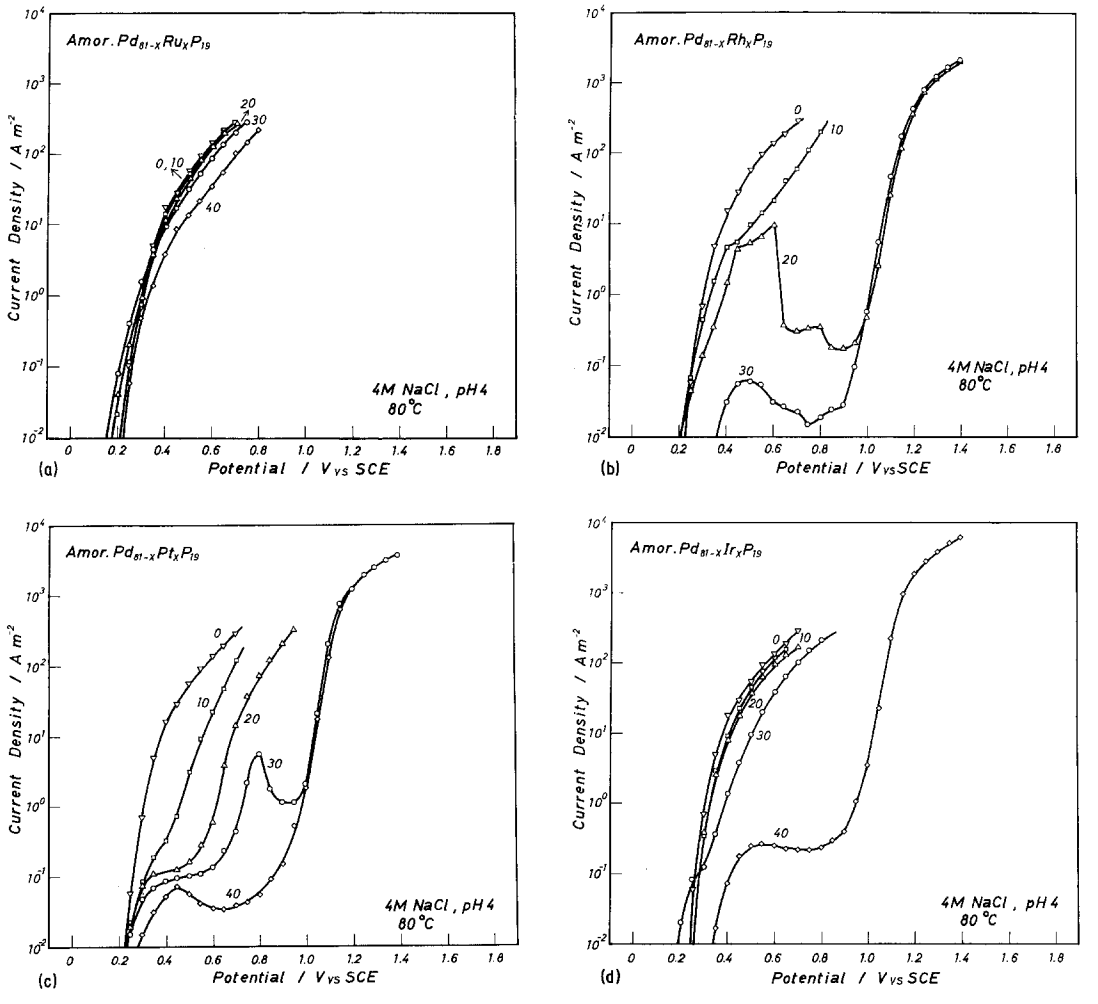

Fig. 2. Potentiostatic anodic polarization curves of amorphous palladium–phosphorus alloys containing varying amounts of a second metallic element measured in 4 mol dm^{-3} NaCl solution of pH 4 and 80° C. The number in the figure denotes the content of the second metallic elements, x, in at %: (a) ruthenium; (b) rhodium; (c) platinum; (d) iridium.

to gas evolution in the potential region higher than about 0.9 V (SCE). The current density in the active region is significantly lower for the alloys containing 30 at % rhodium or 40 at % platinum, suggesting a high corrosion resistance of these alloys. When the latter alloy was potentiostatically polarized for a longer time in the gas evolution region, the current density decreased, indicating a decrease in the gas evolution rate. The amorphous Pd–Ir–P alloy with 40 at % iridium is also passivated by anodic polarization and shows a steep rise in the current density in the potential region higher than about 0.9 V (SCE), as shown in Fig. 2(d). In particular, this alloy exhibits a significantly higher current density in the gas evolution region. Consequently, the addition of rhodium, platinum or iridium can lead to anodic passivation, and when the alloys showed passivation behaviour between 0.6–0.8 V (SCE), they did not dissolve appreciably at high potentials but evolved gases.

Figure 3 shows potentiostatic polarization curves measured by step-wise decrease in the potential from the gas evolution region. Chlorine evolution was observed on the amorphous $Pd_{71}Rh_{10}P_{19}$ and $Pd_{61}Pt_{20}P_{19}$ alloys at high potentials, but they were dissolved following the decrease in the potential below about 1.1 V (SCE). This suggests that the alloys, which could not be passivated by a potential increase (Fig. 2), were not able to form a stable passive film even when they were directly polarized to high potentials in the gas evolution region. Hence both gas evolution and alloy dissolution seemed to occur on these alloys at high potentials. The amorphous $Pd_{81-x}Ir_xP_{19}$ alloys containing not more than 30 at % iridium were more unstable and dissolved vigorously without gas evolution during polarization at high potentials such as 1.4 V (SCE). On the contrary, the amorphous $Pd_{51}Rh_{30}P_{19}$, $Pd_{41}Pt_{40}P_{19}$ and $Pd_{41}Ir_{40}P_{19}$ alloys exhibit no anodic current for active dissolution at potentials below about 1.1 V (SCE) but show a cathodic current due to reduction of chlorine formed previously during polarization in the gas evolution region. This indicates that polarization of these alloys in the gas evolution region results in the formation of a stable passive film, on which chlorine evolution takes place. It can, therefore, be concluded that the addition of the second platinum group metals is beneficial in improving the corrosion resistance because it favours passivation due to an improvement of the stability of the surface film.

On the other hand, an amorphous alloy can be prepared by rapid quenching from the molten state even if silicon is substituted for phosphorus. The influence of silicon on the passivation behaviour of the alloys was also examined. Figure 4 shows potentiostatic polarization curves for four amorphous $Pd_{56}Rh_{25}P_xSi_{19-x}$ alloys. The amorphous $Pd_{55}Rh_{25}P_{19}$ alloy exhibits a low current density in both the active and passive regions below potentials for gas evolution. When a portion of the phosphorus is replaced by silicon the current density in the active region increases. The anodic current density of amorphous $Pd_{56}Rh_{25}Si_{19}$ alloy is still higher than that of amorphous

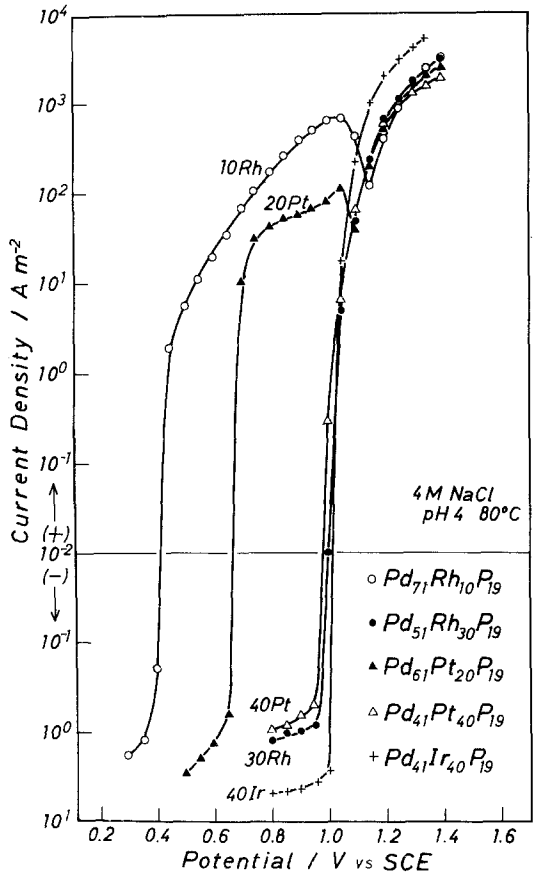

Fig. 3. Potentiostatic polarization curves of amorphous Pd–P alloys measured by the step-wise decrease in the potential from 1.4 V (SCE) in a 4 mol dm^{-3} solution of pH 4 and 80° C.

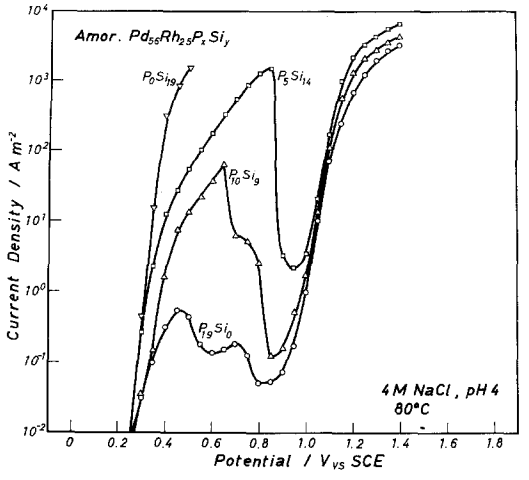

Fig. 4. The effect of silicon content on potentiostatic anodic polarization curves of amorphous $Pd_{56}Rh_{25}P_xSi_y$ alloys measured in 4 mol dm^{-3} NaCl solution of pH 4 and 80° C.

$Pd_{81}P_{19}$ alloy without rhodium, although it is lower than that of cystalline pure palladium (Fig. 1). The polarization curves of the $Pd_{56}Rh_{25}Si_{19}$ alloy could not be measured at potentials above 0.5 V (SCE) since this alloy dissolved rapidly. These results imply that it is difficult to improve the corrosion resistance of amorphous palladium-base alloys with silicon, cf. the amorphous iron-silicon alloys [25, 26].

In order to examine the corrosion resistance in the gas evolution region of the amorphous alloys which were passivated by anodic polarization, their corrosion rates during galvanostatic polarization at 1000 Am^{-2} were measured in 4 mol dm^{-3} NaCl solution of pH 4 and 80° C. The pH of the solution in the anode compartment after the corrosion test was also measured. For comparison, the corrosion rates of crystalline pure ruthenium, rhodium, palladium, iridium and platinum were also measured. The results are summarized in Table 1. The pH of the solution in the anode compartment was signficantly lowered by galvanostatic polarization, and hence these solutions were considerably aggressive in comparison with the solution currently used in the chlor alkali industry. The pH decrease of the anolyte during electrolysis of the static sodium chloride solution is well known [27, 28] to be due to disproportionation reactions of dissolved chlorine with water; e.g., $Cl_2 + H_2O = HClO + HCl$. The corrosion rate for pure palladium is extremely high as can also be seen in Fig. 1. Nevertheless, amorphous palladium-base alloys containing a sufficient amount of rhodium, platinum or iridium show low corrosion rates similar to crystalline pure rhodium, platinum or iridium. When the corrosion rate of the corresponding crystalline alloys were examined by potentiostatic polarization at 1.25 V (SCE), those of crystalline $Pd_{50}Ir_{50}$ and $Pd_{41}Ir_{40}P_{19}$ alloys were 274 and 134 g m^{-2} h^{-1}, respectively, while that of amorphous $Pd_{41}Ir_{40}P_{19}$ alloy was less than 0.1 g m^{-2} h^{-1}.

Table 1. Corrosion rate of amorphous Pd–P alloys and crystalline pure metals estimated from the weight loss during galvanostatic anodic polarization at 1000 Am^{-2} in 4 mol dm^{-3} NaCl solution at 80° C. The pH of the solution in the anode compartment was measured before and after polarization

Electrode	*Testing time* (h)	*pH*		*Corrosion rate* (g m^{-2} h^{-1})
		Before test	*After test*	
Amorphous alloy				
$Pd_{61}Rh_{20}P_{19}$	25	4	1.35	0.00
$Pd_{51}Rh_{30}P_{19}$	25	4	1.3	0.00
$Pd_{51}Pt_{30}P_{19}$	25	4	1.3	0.02
$Pd_{41}Pt_{40}P_{19}$	25	4	1.3	0.01
$Pd_{41}Ir_{40}P_{19}$	25	4	1.35	0.18
Crystalline pure metal				
Pd	0.2	4	2.7	2027.08
Rh	25	4	1.1	0.02
Pt	25	4	1.2	0.03
Ir	25	4	1.2	0.02
Ru	25	4	1.1	0.18

3.2. *Catalytic activities for evolution of chlorine and oxygen*

Three kinds of corrosion-resistant amorphous palladium-based alloys were used to estimate their catalytic activities for evolution of chlorine and oxygen. They were the $Pd_{51}Rh_{30}P_{19}$, $Pd_{41}Pt_{40}P_{19}$ and $Pd_{41}Ir_{40}P_{19}$ alloys. The galvonstatic polarization curves were measured in both 4 mol dm^{-3} NaCl and 1 mol dm^{-3} Na_2SO_4 solutions. The results are shown in Figs. 5–7. The curves shown in (a) and (b) in each figure correspond to anodic polarization curves measured in 4 mol dm^{-3} NaCl and 1 mol dm^{-3} Na_2SO_4 solutions, respectively. As shown in Fig. 5(b), the anodic polarization curves of amorhpous $Pd_{51}Rh_{30}P_{19}$ alloy measured in 1 mol dm^{-3} Na_2SO_4 solution is not very different from that of pure rhodium, and hence the overvoltage of the alloy for oxygen evolution maybe almost the same as that of pure rhodium. However, the anodic polarization curves of the amorphous alloy measured in 4 mol dm^{-3} NaCl solution apparently differs from that of pure rhodium as shown in Fig. 5(a). It can, therefore, be concluded that the electrocatalytic activity of the amorphous $Pd_{51}Rh_{30}P_{19}$ alloy for evolution of chlorine is higher than that of pure rhodium. On the other hand, the electrocatalytic activities of the amorphous $Pd_{41}Pt_{40}P_{19}$ alloy for evolution of both chlorine and oxygen are higher than those of pure platinum as shown in Fig. 6. As shown in Fig. 7, the activity of the amorphous $Pd_{41}Ir_{40}P_{19}$ alloy for gas evolution in 4 mol dm^{-3} NaCl solution is higher than that of pure iridium, whereas the activity of the alloy in 1 mol dm^{-3} Na_2SO_4 solution is lower than that of pure iridium.

The current densities at 1.15 V (SCE) were estimated from the galvanostatic polarization

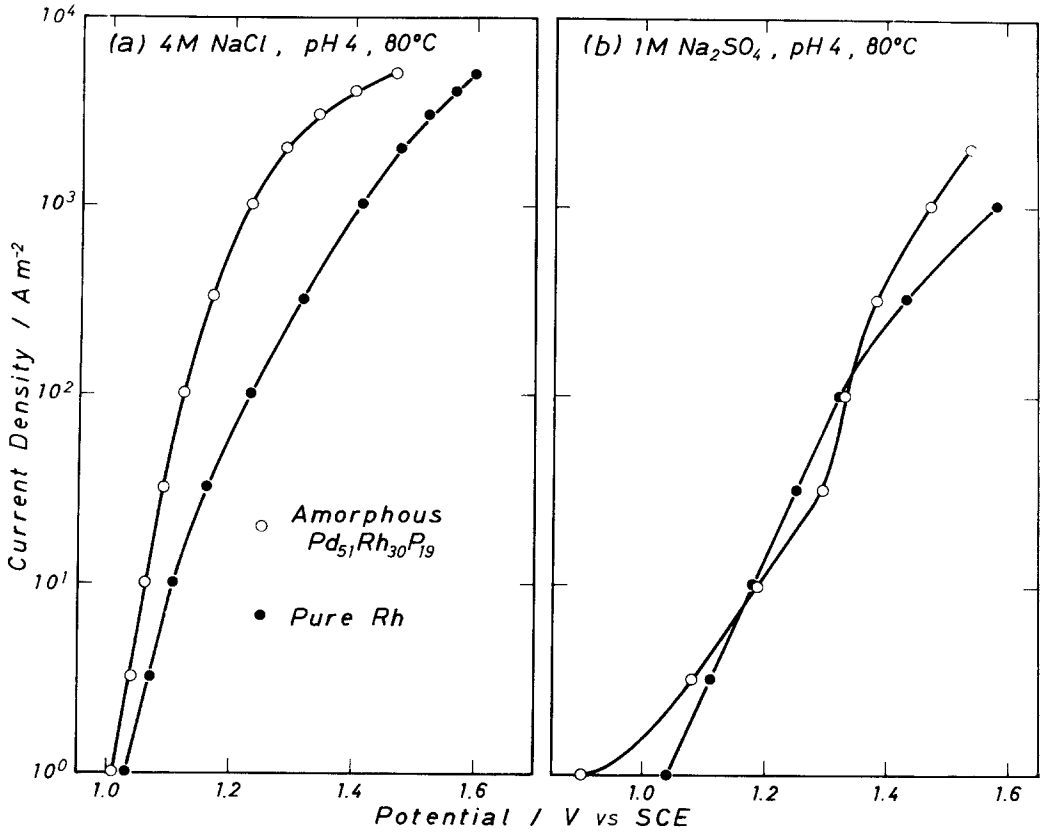

Fig. 5. Galvanostatic anodic polarization curves of amorphous $Pd_{51}Rh_{30}P_{19}$ alloy and crystalline pure rhodium measured in 4 mol dm^{-3} NaCl solution of pH 4 and 80° C (a) and in 1 mol dm^{-3} Na_2SO_4 solution of pH 4 and 80° C.

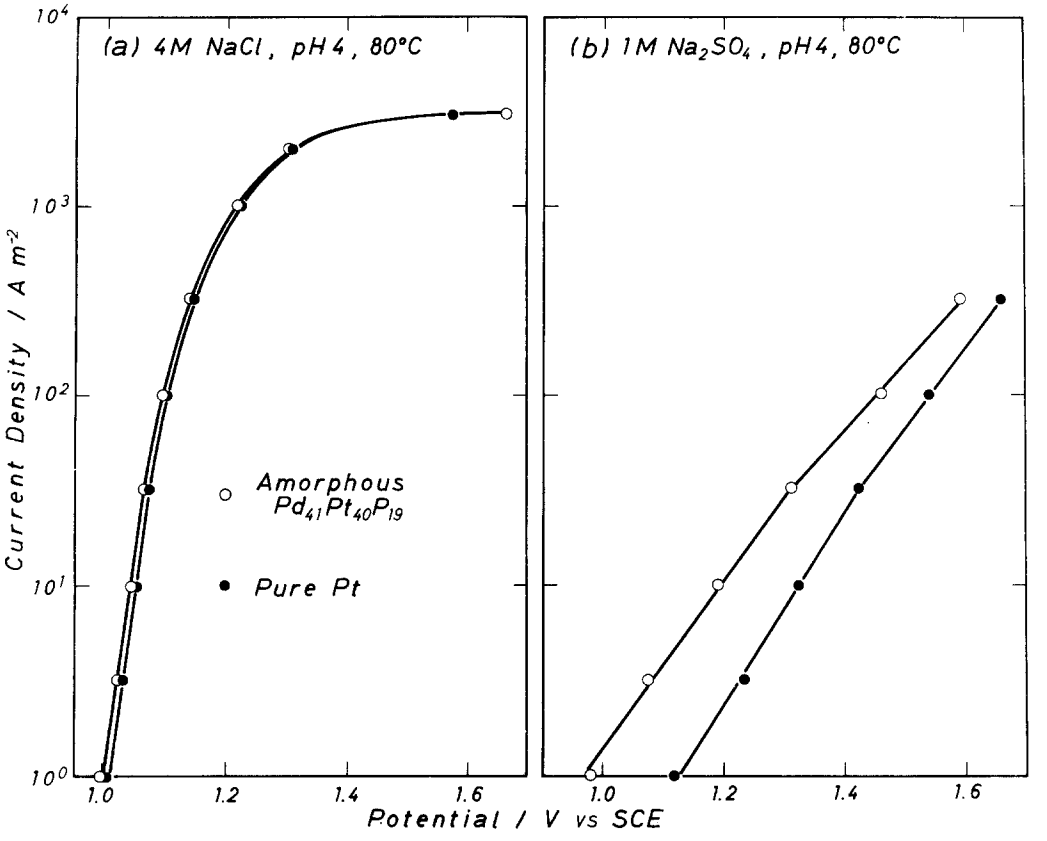

Fig. 6. Galvanostatic anodic polarization curves of amorphous $Pd_{41}Pt_{40}P_{19}$ alloy and crystalline pure platinum measured in 4 mol dm^{-3} NaCl solution of pH 4 and 80° C (a) and in 1 mol dm^{-3} Na_2SO_4 solution of pH 4 and 80° C (b).

curves and are summarized in Table 2, which also includes the current densities estimated from the galvanostatic polarization curves of crystalline platinum group metals and the RuO_2/Ti electrode. Crystalline pure palladium did not evolve gases in 4 mol dm^{-3} NaCl solution of pH 4 and 80° C because of rapid dissolution, and hence the comparison of the activities for gas evolution of palladium with other platinum group metals was carried out in 2 mol dm^{-3} NaCl and 1 mol dm^{-3} Na_2SO_4 solution of pH 4 and 30° C. Among the platinum group metals palladium shows the highest current density in 2 mol dm^{-3} NaCl solution but there is a low current in 1 mol dm^{-3} Na_2SO_4 solution, suggesting that palladium has the highest electrocatalytic activity for chlorine evolution, but is not an effective anode for oxygen evolution. This clearly indicates that palladium would be the best anode for chlorine evolution if it were corrosion resistant. On the other hand, ruthenium exhibits the second highest electrocatalytic activity for gas evolution in sodium chloride solutions and is most active in 1 mol dm^{-3} Na_2SO_4 solutions, suggesting that the gas evolved on the ruthenium anode in sodium chloride solutions will be contaminated with a high concentration of oxygen. Accordingly, even if the corrosion resistance is improved by preparation of amorphous ruthenium-based alloys, they may not be an effective anode for electrolysis of sodium chloride solutions. The platinum group metals other than palladium and ruthenium have low activities for gas evolution, and these metals cannot be used as the anode for chlorine manufacture. On the other hand, the electrocatalytic activity for chlorine evolution of amorphous $Pd_{41}Ir_{40}P_{19}$ alloy is significantly higher than those of crystalline pure platinum group metals and is even higher than that of the RuO_2/Ti electrode. In addition, the electrocatalytic activity for

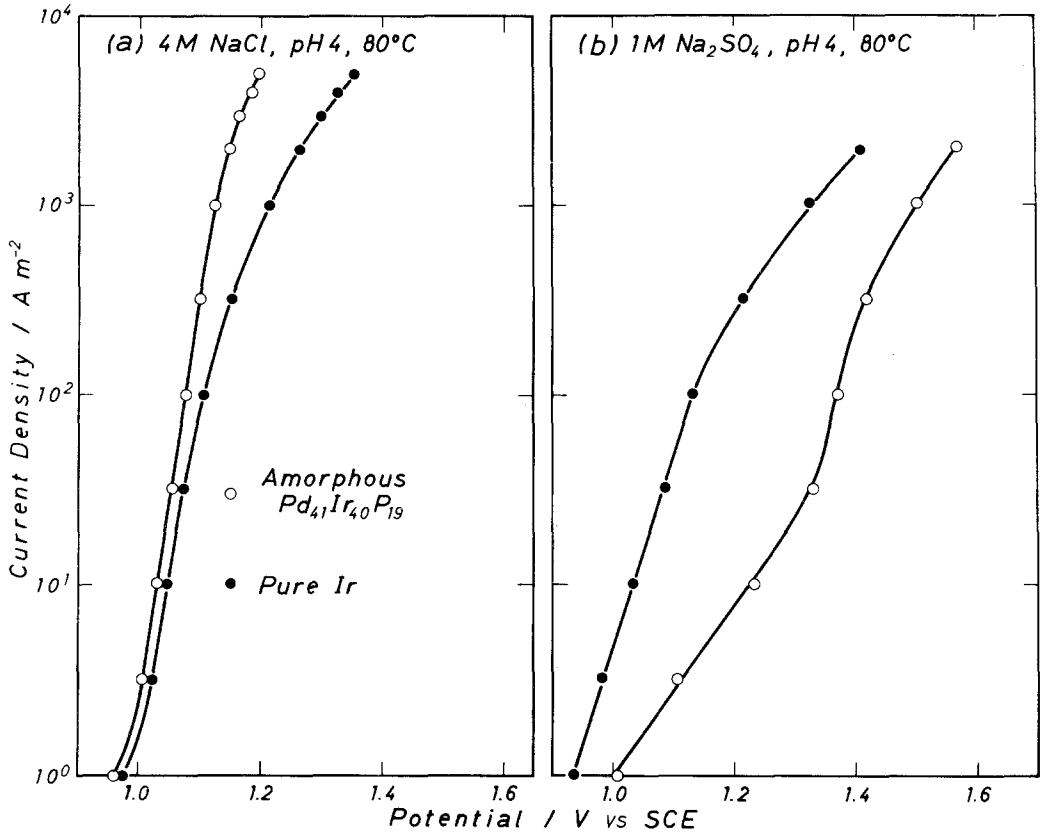

Fig. 7. Galvanostatic anodic polarization curves of amorphous $Pd_{41}Ir_{40}P_{19}$ alloy and crystalline pure iridium measured in 4 mol dm^{-3} NaCl solution of pH 4 and 80° C and in 1 mol dm^{-3} Na_2SO_4 solution of pH 4 and 80° C.

oxygen evolution of the amorphous $Pd_{41}Ir_{40}P_{19}$ alloy is considerably lower than those of pure iridium and the RuO_2/Ti electrode, and those of the other amorphous alloys are also comparable to the activities of platinum and rhodium for oxygen evolution. Accordingly,

Table 2. Current densities for amorphous ternary palladium–phosphorus alloys, crystalline platinum group metals and the RuO_2/Ti electrode estimated from galvanostatic polarization curves measured in NaCl and Na_2SO_4 solutions of pH 4.

Electrode	*Current density* (Am^{-2})			
	80° C, 1.15 V (SCE)		30° C, 1.30 V (SCE)	
	4 mol dm^{-3} NaCl	1 mol dm^{-3} Na_2SO_4	2 mol dm^{-3} NaCl	1 mol dm^{-3} Na_2SO_4
Amorphous alloy				
$Pd_{51}Rh_{30}P_{19}$	220	7	–	–
$Pd_{41}Pt_{40}P_{19}$	400	6	–	–
$Pd_{41}Ir_{40}P_{19}$	2000	5	–	–
Crystalline metal				
Ru	1300	1400	1000	495
Rh	26	6	9	3
Pd	–	16	1630	4
Ir	340	150	280	41
Pt	340	1	190	1
RuO_2/Ti	1700	340	–	–

the oxygen content in the gas evolved on these amorphous alloys in sodium chloride solutions may be very low. It should be emphasized that the amorphous $Pd_{41}Ir_{40}P_{19}$ alloy has a high activity for chlorine evolution and low activity for oxygen evolution in comparison with all the platinum group metals other than palladium.

As mentioned above, chlorine evolution occurs on the passive film which is simultaneously responsible for the corrosion resistance of the alloys. The chlorine evolution on the passive film sometimes results in degradation of the passive film with a consequent lowering of the activity for gas evolution and, in the worst case, depassivation [22]. It is, therefore, necessary to examine the stability of the electrocatalytic activity of the alloys for chlorine evolution. Hence the change in the electrode potential during galvanostatic polarization at 2000 Am^{-2} was measured and is shown in Fig. 8. The figure includes the potential–time curves of crystalline pure rhodium, platinum and iridium for comparison. The change in the potential of the amorphous palladium-based alloys is dependent on the additional element, (rhodium, platinum or iridium); the amorphous $Pd_{41}Pt_{40}P_{19}$ alloy shows the same potential as pure platinum after 0.5 h, and the potential of the amorphous $Pd_{51}Rh_{30}P_{19}$ alloy becomes close to that of pure rhodium after 1.5 h, indicating that the quality of the passive films on these alloys was gradually changed by polarization toward that of the films on crystalline pure platinum and rhodium. On the contrary, though the electrode potential of the amorphous $Pd_{41}Ir_{40}P_{19}$ alloy is close to that of pure iridium, it gradually decreases and becomes 0.06 V less noble than that of pure iridium after 2.5 h. The Tafel slopes for the amorphous $Pd_{41}Ir_{40}P_{19}$ alloy and crystalline pure iridium for chlorine evolution estimated from Fig. 7 were 0.048 and 0.050 V $decade^{-1}$, respectively. Accordingly, if the mechanism for chlorine evolution is unchanged after prolonged polarization, the rate of chlorine evolution on the amorphous $Pd_{41}Ir_{40}P_{19}$ alloy anode at a constant cell voltage will be more than one order of magnitude higher than that on the crystalline iridium anode. This difference in the activities is larger than that shown in Table 2 which were estimated from the galvanostatic polarization curves obtained each polarization for 300 s at each current density.

4. Discussion

An attempt was made at transformation from the crystalline state to the amorphous state to improve the corrosion resistance of palladium while maintaining the very high electrocatalytic activity as the anode for chlorine evolution. As shown in Fig. 1, however, amorphous Pd–P and Pd–Si alloys exhibit high current density due to dissolution similar to pure palladium. This implies that the transformation to the amorphous structure alone is not effective in improving the corrosion resistance. As shown in Fig. 2, however,

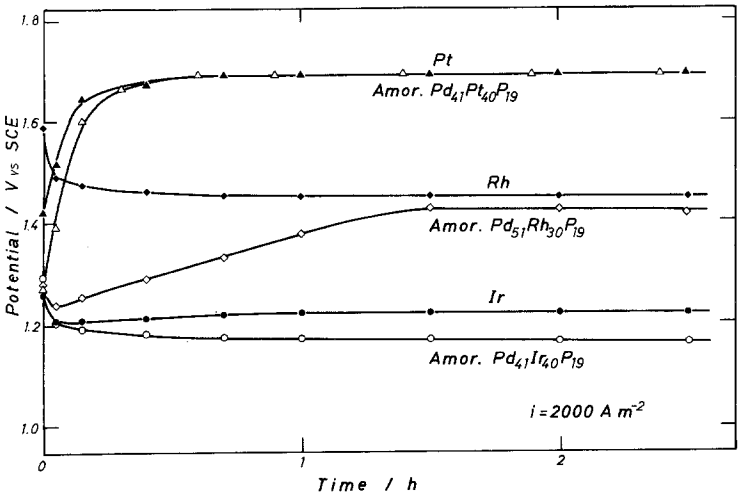

Fig. 8. Potential–time curves of amorphous Pd–P alloys and pure metals measured by galvanostatic anodic polarization at 2000 Am^{-2} in 4 mol dm^{-3} NaCl solution of pH 4 and 80° C.

the ternary amorphous palladium-based alloys containing sufficient quantities of rhodium, platinum or iridium are passivated by anodic polarization and evolve gases in the potential region higher than about 0.9 V (SCE). The beneficial effect of the addition of the second metallic element in improving the corrosion resistance has also been found for amorphous iron-based alloys [17–19]; the corrosion rate of binary amorphous iron-metalloid alloys is higher than that of pure iron, but addition of chromium, molybdenum, nickel, etc. significantly lowers the corrosion rate.

As shown in Table 1, the amorphous Pd–Rh–P, Pd–Pt–P and Pd–Ir–P alloys possess high corrosion resistance during the electrolysis of NaCl solutions at high current densities. On the other hand, the stepwise decrease in the potential for the corrosion-resistant alloys from the gas evolution region to the active dissolution region reveals the cathodic current instead of active dissolution at potentials lower than about 1.0 V (SCE) (Fig. 3), indicating the formation of a stable passive film in the gas evolution region. This is responsible for high corrosion resistance of the amorphous alloys in the gas evolution region. The high corrosion resistance of these amorphous alloys is not attributable only to the beneficial effect of the addition of rhodium, platinum or iridium. The corrosion rate of crystalline $Pd_{50}Ir_{50}$ and $Pd_{41}Ir_{40}P_{19}$ alloys were more than three orders of magnitude higher than that of the amorphous $Pd_{41}Ir_{40}P_{19}$ alloy, indicating the beneficial effect of the formation of the amorphous structure. Hashimoto *et al.* [29], in reporting the corrosion behaviour of amorphous and crystalline alloys, have stated that the high corrosion resistance of the amorphous alloy in comparison with the crystalline alloy of the same composition is partly attributable to the chemically homogeneous, single phase nature of the amorphous alloy which allows the formation of a uniform, highly protective passive film.

The metalloids contained in the alloys also affected the passivating ability; substitution of silicon for phosphorus decreased the passivating ability. According to Hashimoto *et al.* [26], phosphorus is most effective among the metalloids in accelerating passivation. Furthermore, the formation of polyoxyanions such as phosphate, silicate or borate in the passive film is detrimental to the corrosion resistance, but phosphate, unlike silicate and borate, is not retained in the stable passive film [30].

It can, therefore, be concluded that the transformation to the amorphous structure and the addition of rhodium, iridium or platinum are both effective in forming the stable passive film on the amorphous phosphorus-bearing palladium-based alloys which provide the high corrosion resistance in hot concentrated sodium chloride solutions.

The elctrocatalytic activities for evolution of chlorine and oxygen are also greatly affected by the alloy composition. Since the stable passive film is formed on the amorphous alloys in the gas evolution region, the gas evolution reaction appears to occur at the film-solution interface. On the contrary, if chlorine were evolved directly on the alloy surface due to leakage of the solution through defects of the film, high corrosion resistance would not be expected. As shown in Figs. 5–7 and Table 2 the electrocatalytic acitivities for chlorine evolution of the amorphous $Pd_{51}Rh_{30}P_{19}$, $Pd_{41}Pt_{40}P_{19}$ and $Pd_{41}Ir_{40}P_{19}$ alloys are higher than those of pure rhodium, platinum and iridium, respectively. This may be due to the fact that the passive films formed on the amorphous alloys are different from those on crystalline pure metals in nature owing to the presence of palladium. As shown in Fig. 8, however, prolonged galvanostatic polarization of the amorphous $Pd_{41}Pt_{40}P_{19}$ and $Pd_{51}Rh_{30}P_{19}$ alloys leads to an increase in the potentials, to those of crystalline pure platinum and rhodium. This may be interpreted in terms of the change in the composition of the passive film to those consisting mainly of platinum or rhodium as cations which are less active for chlorine evolution. On the other hand, the amorphous $Pd_{41}Ir_{40}P_{19}$ alloy maintains a high activity for chlorine evolution during prolonged polarization due probably to the high stability of the passive film formed initially on the alloy. A detailed investigation to correlate the electrocatalytic activity with the composition and thickness of the surface film will be reported subsequently.

It is worth noting from the practical point of view that the amorphous $Pd_{41}Ir_{40}P_{19}$ alloy has the stable, high electrocatalytic activity for

chlorine evolution, the high overpotential for oxygen evolution and the high corrosion resistance in hot concentrated NaCl solutions.

References

[1] A. Yokoyama, H. Komiyama, H. Inoue, T. Masumoto and H. M. Kimura, *Scripta Met.* **15** (1981) 365.
[2] *Idem, J. Catalysis* **68** (1981) 355.
[3] *Idem,* Rapidly Quenched Metals in 'Proceedings of the 4th Interntional Conference on Rapidly Quenched Metals', Vol. II, (edited by T. Masumoto and K. Suzuki) Japan Institute of Metals, Sendai (1982) p. 1419.
[4] A. Kawashima and K. Hashimoto, *ibid.* Japan Institute of Metals, Sendai (1982) p. 1427.
[5] A. T. Kuhn, 'Industrial Electrochemical Processes', Elsevier, Amsterdam (1971).
[6] O. De Nora, *Chem. Ind. Techn.* **42** (1970) 222.
[7] B. V. Ershier, *Z. Fiz. Khim.* **18** (1944) 131.
[8] G. A. Tedoradse, *Z. Fiz. Khim.* **33** (1959) 129.
[9] J. S. Mayell and S. H. Langer, *Electrochim. Acta* **9** (1964) 1411.
[10] J. Llopis, J. M. Gamboa and J. M. Alfayate, *Electrochim. Acta* **12** (1967) 57.
[11] 'Soda Handbook', Japan Soda Industry Association, Tokyo, (1975) p. 224.
[12] M. Takahashi, *Soda and Chlorine* **26** (1975) 267.
[13] Ya. M. Kolotyrkin, *Denki Kagaku* **47** (1979) 390.
[14] General Electric Co. Ltd. Japanese Patent 54-97581, 54-112398 (1979).
[15] M. Naka, K. Hashimoto and T. Masumoto, *Corrosion* **32** (1976) 146.
[16] K. Hashimoto, M. Kasaya, K. Asami and T. Masumoto, *Corros. Eng. (Boshoku Gijutsu)* **26** (1977) 445.
[17] M. Naka, K. Hashimoto and T. Masumoto, *J. Non-Cryst. Solids* **29** (1978) 61.
[18] *Idem, ibid.* **31** (1979) 257.
[19] *Idem, ibid.* **34** (1979) 347.
[20] M. Naka, K. Hashimoto, A. Inoue and T. Masumoto, *ibid.* **31** (1979) 347.
[21] T. Masumoto and R. Maddin, *Acta Met.* **19** (1971) 725.
[22] M. Hara, K. Hashimoto and T. Masumoto, *Electrochim. Acta* **25** (1980) 1215.
[23] M. Hara, K. Asami, K. Hashimoto and T. Masumoto, *Electrochim. Acta* **25** (1980) 1091.
[24] D. Galizzioli, F. Tantardini and S. Trasatti, *J. Appl. Electrochem.* **4** (1974) 57.
[25] M. Naka, K. Hashimoto and T. Masumoto, *J. Non-Cryst. Solids* **28** (1978) 403.
[26] K. Hashimoto, M. Naka, K. Asami and T. Masumoto, *Corros. Eng. (Boshoku Gijutsu)* **27** (1978) 279.
[27] A. A. Jakowkin, *Z. physik. Chem.* **29** (1899) 61.
[28] M. Takahashi, *Soda and Chlorine* **29** (1978) 379.
[29] K. Hashimoto, K. Osada, T. Masumoto and S. Shimodaira, *Corros. Sci.* **16** (1976) 71.
[30] K. Hashimoto, K. Asami, M. Naka and T. Masumoto, *Corros. Eng. (Boshoku Gijutsu)* **28** (1979) 271.